Medium and high grazing angle sea-clutter effects on the radar performance located on a drone

Hamza Bounaceur, Ali Khenchaf, Jean-Marc Le Caillec

Medium and high grazing angle sea-clutter effects on the radar performance located on a drone

Hamza Bounaceur
Lab-STICC UMR CNRS 6285
ENSTA Bretagne
Brest, France
hamza.bounaceur@ensta-bretagne.org

Ali Khenchaf
Lab-STICC UMR CNRS 6285
ENSTA Bretagne
Brest, France
ali.khenchaf@ensta-bretagne.fr

Jean-Marc Le Caillec
Lab-STICC UMR CNRS 6285
IMT Atlantique
Brest, France
jm.lecaillec@imt-atlantique.fr

Abstract— **In recent years, small craft used for drug trafficking, smuggling, human trafficking and piracy have posed a growing threat to ocean observations and maritime traffic surveillance. In order to combat such threats, microwave radars have been widely used, for maritime surveillance and target reconnaissance tasks, due to their capabilities to operate in all weathers and day and night. However, maritime radars, and particularly those carried on aircraft (such as drones), are confronted with disturbances due to sea clutter which has a strong impact on the detection function, in particular for observations at very grazing angles. Despite that airborne maritime radars typically operate at low grazing angles, from necessity or to achieve the best detection performance, it has also become important to better understand the characteristics of clutter observed at medium and higher grazing angles to undertake maritime reconnaissance using radar embedded on drones. Thus, with a view to better control of sea clutter in a context of observation via a drone with the development of functions for detecting, locating and tracking targets present in a maritime environment, this paper offers a summary of different modelling and characterization of sea clutter in grazing to very grazing configurations.**

Keywords—Maritime radar, Drone, Sea clutter, K-distribution, Grazing angle

I. INTRODUCTION

Thanks to its advantages, airborne maritime radar has become an important means of maritime target detection [1]. the global observation link is considered with at the same time, the considering of the characteristics of the carrier (frequency of 10 GHz, its movement, ...), the atmospheric propagation channel, the sea clutter and the signals received at the level of the wearer. By considering an observation chain from a drone, with the aim of detecting and following small moving targets in a maritime environment, one of the fundamental steps relates to the fine characterization of the sea clutter [2]. the signal reflected by a maritime target will be drowned in the moving clutter and the problem therefore boils down to the detection of a target in a non-stationary environment. These detection problems are compounded by the fact that sea conditions can severely inhibit detection performance, especially when the radar observes relatively small targets, where the probability of detection is reduced due to the weak targets radar cross section (RCS).

To better understand the characteristics of sea clutter, several methodologies have been developed in the literature, both via electromagnetic, empirical and statistical models. K distribution model [3] appears as the most physical applicable to the amplitude statistics of sea clutter. It has two parameters: the shape parameter (v) linked with the power of the clutter and the scale parameter (b) that gives an indication of how "peaked" the clutter is.

The main goal in this paper would be the analysis of shape and scale parameter of k distribution clutter as a function of the observation geometry (from moderately grazing to very grazing). We will focus on description of the target detection performance of an airborne surface surveillance radar in the presence of medium and higher grazing angle sea-clutter at X-Ku band, horizontal and vertical polarization. Thus, in order to examine the effect of grazing angle on ocean backscatter, different scenarios will be considered in the context of different simulations with different grazing angles.

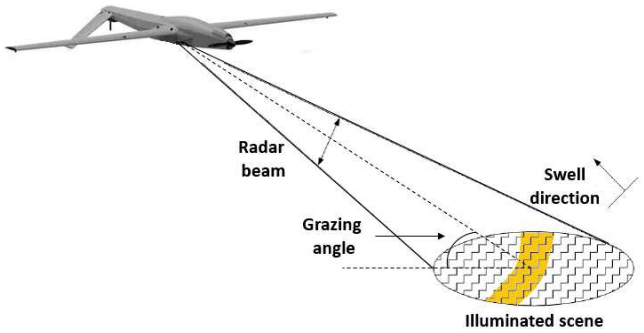

Fig. 1 The viewing geometry of radar located on a drone illuminate an area of the sea with a given grazing angle

II. MEDIUM AND HIGH GRAZING ANGLE NORMALISED RCS MODELS

The most fundamental characteristic of sea clutter remains its average reflectivity or normalized radar cross section σ^0 (NRCS). It is defined as the total RCS (σ) of the scatterers in the illuminated patch, normalized by the area (A_c) of the patch. The always changing and complex nature of the sea surface implies that the RCS of the return will fluctuates widely around the mean value as determined by σ^0. For the latter, there are several radar parameters and a number of environmental conditions that define it such as sea state, wind velocity, grazing angle, transmit power, carrier frequency, distance between radar and sea clutter area element, area of illumination and polarization. It is measured in units of dB m²/m²:

$$\sigma^0 = \frac{\sigma}{A_c} \quad (1)$$

The area of every area element (A_c) can be computed as below.

$$A_c = \alpha \frac{R\rho\varphi_{az}}{cos(\theta_{gr})} \quad (2)$$

Where R is the distance between radar and sea clutter area element, φ_{az} is the radar beam width of 3 dB, in radian form and θ_{gr} is the grazing angle. The range resolution ρ, is related to the radar pulse bandwidth, B by $\rho = \frac{c}{2B}$. The factor α accounts for the actual compressed pulse shape and the azimuth beamshape, including the range and azimuth sidelobes. For a rectangular shaped pulse and beamshape, $\alpha = 1$, while for a Gaussian-shaped beam and rectangular pulse, $\alpha = 0.753$.

Then we can redefine (1) as:

$$\sigma^0 = \frac{\sigma}{\alpha R \rho \varphi_{az}} cos(\theta_{gr}) \quad (3)$$

The grazing angle θ_{gr} is the angle from the surface of the ocean to the main axis of the illuminating beam as illustrated in Figure 1. For a nominally average flat surface, such as the sea, it can be defined in terms of the radar height and slant range.

$$\theta_{gr} = arcsin\left(\frac{h}{R} + \frac{h^2}{2r_e R} - \frac{R}{2r_e}\right) \quad (4)$$

h is the height of the radar, r_e is the effective Earth's radius and R is the slant range. For routine calculations at sea level, $r_e = \frac{4}{3r}$, where r is the true earth radius.

Figure 2 (adapted from reference [4]) illustrates the general relationship between the normalized backscatter reflectivity σ^0 and the grazing angle θ_{gr}.

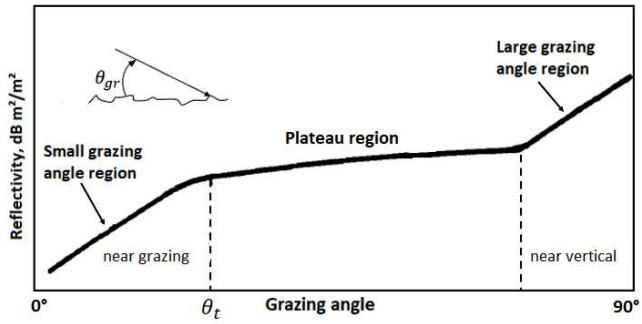

Fig. 2 Idealized relationship sea clutter reflectivity and grazing angle

Three regions are identified:

- Low grazing angle region, below some critical angle (~10°, depending on the roughness) the reflectivity reduces rapidly with smaller grazing angles.
- Flat or plateau region in which the normalized reflectivity does not vary strongly with grazing angle.
- High grazing angle region, the normalized reflectivity increases sharply with grazing angle in this region.

There are various empirical models for the normalized clutter reflectivity that are used by radar designers. Tables of σ^0 for different radar frequencies, grazing angles and sea states and for horizontal and vertical polarizations are given in [5]. The models are mainly applicable to grazing angle < 10°. At higher grazing angles, the scattering mechanisms are less complex but nevertheless empirical models are often used. Notable among these are the Technology Service Corporation model (TSC) [6], it is valid in between 0.5 GHz and 35 GHz and it claims validity for all grazing angle from 0° to 90°. Another approach to modelling σ^0 at grazing angles above about 30° is described by Ulaby et al. [7]. Recently, a model has been developed at NRL [8], can be used for Radar frequencies from 0.5 GHz to 35 GHz and grazing angles in between 0.1° and 60°. The comparison of the predictions obtained with these three models between 30° and 60° grazing angle in X-band is shown in Figure 3.

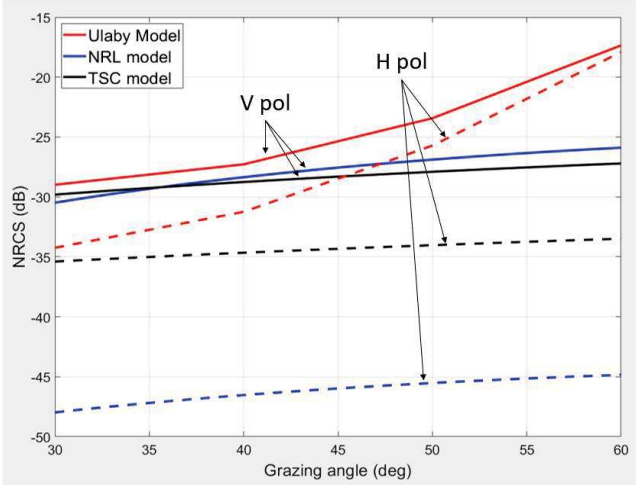

Fig. 3 NRCS as a function of grazing angle (30° - 60°)

The analysis of this phenomenon (normalized backscatter reflectivity) is quite complex, and the simulation results of the different models do not always coincide. Consequently, the models proposed can only be approximate. At least, it can be seen that the normalized reflectivity of sea clutter increases with increasing grazing angle and the HH reflectivity is generally lower than VV over a range of grazing angles. So, when operating at higher grazing angles especially in VV polarization, the clutter return increases in intensity and will cover target echo and reduces the performance that can be achieved by traditional non-coherent detection methods.

III. COMPOUND K-DISTRIBUTION MODEL AND PARAMETER ESTIMATION

A. Shape parameter at low grazing angle

Because of spikes, sea clutter is generally described by the statistical distribution with long tail, such as the compound K distribution (CKD) as it was shown to be a matched fit to sea clutter amplitude data under various conditions. The CKD is a compound distribution that is used to model the speckle and texture sea clutter amplitude structures. The speckle is a small-scale structure that accounts for the reflections from multiple scatters with short temporal decorrelation period, while the texture is a large-scale structure that modulates the speckle component.

$$P(x) = \frac{2.b}{\Gamma(v)} . (\frac{b.x}{2})^v . k_{v-1}(b.x) \quad (5)$$

Where $K_v(x)$ is the modified Bessel function of order ν.

The CKD amplitude model is characterized by the shape parameter ν and scale parameter b. The shape parameter has a direct relation with the average number of contributing scatterers on the sea surface [9], and gives an indication of how "peaked" the clutter is. As such, for little values of ν, the clutter will have large amplitude peaks, while for large values of ν, it will be relatively smoothed. For various values of ν, the pdf of K distribution is plotted in Figure 4.

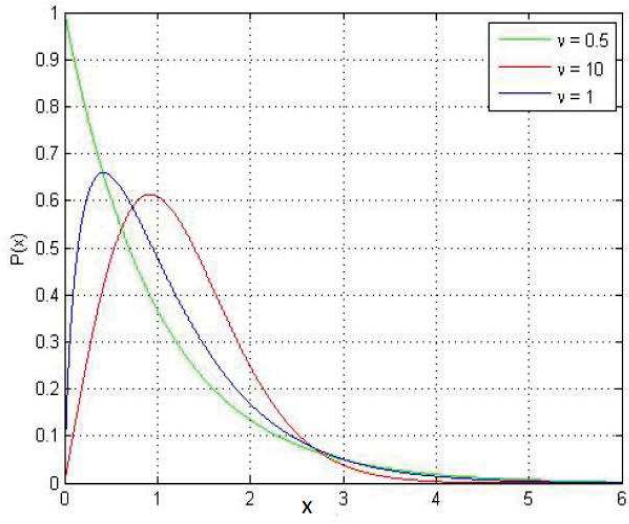

Fig. 4 K distribution PDF for scale parameter set to 1 and different shape.

When the K distribution model was developed through the analysis of experimental airborne radar data [10], an empirical model for the dependence of the shape parameter on radar, environmental and geometric parameters has been developed through the analysis of experimental data at X-band (9–10 GHz), but from the limited data that was available, it is believe to work reasonably well from 5 to 35 GHz. Until recently, it is the only model suitable for modelling the K distribution shape for grazing angles θ_{gr} in the range 0.1° to 10° [11]:

$$log_{10}(v) = \frac{2}{3} log_{10}(\theta_{gr}) + \frac{5}{8} log_{10}(A_c) - K_{pol} - \frac{\cos(2\varphi_{sw})}{3} \quad (6)$$

Where;
θ_{gr} Grazing angle in degrees
A_c Radar resolved area
φ_{sw} Aspect angle with respect to the swell direction
K_{pol} Polarization dependent parameter, takes the value 1.39 for vertical polarization and 2.09 for horizontal

Equation (6) shows that the spikiness of the clutter is impacted by the radar collection parameters such as grazing angle, in addition to the polarization and the direction of the sea swell. The simulation of the shape parameter ν at 0.1°, 1°, 5° and 10° is presented in Figure 5. It is clear that its value increases with grazing angle for both HH and VV polarizations, although the values for VV polarization are high in all cases. Also, the shape parameter has a generally sinusoidal variation with azimuth angle, aligned to the wind direction, with peaks in the upwind and downwind directions.

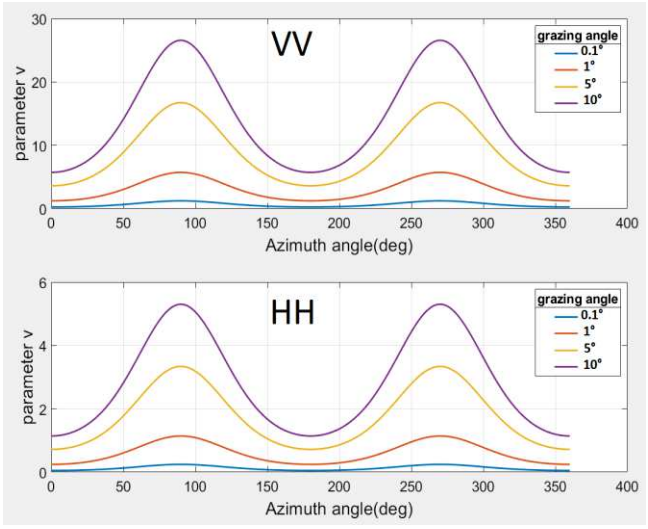

Fig. 5 K shape parameter ν as a function of grazing and azimuth angle

Some additional work has been done to extend the empirical model for ν. For example, Watts and Wicks [12] reported further analysis of the K distribution shape parameter. Their model is given as:

$$log_{10}(v) = A' log_{10}(\theta_{gr}) + B' log_{10}(A_c) + C' \quad (7)$$

With the values of A', B' and C' given in [11].
If we define the sum and difference shape values as

$$v_{sum}(\theta_{gr}) = \frac{v_{US}(\theta_{gr}) + v_{CS}(\theta_{gr})}{2} \quad (8)$$

$$v_{diff}(\theta_{gr}) = \frac{v_{US}(\theta_{gr}) - v_{CS}(\theta_{gr})}{2}$$

$v_{US}(\theta_{gr})$ and $v_{CS}(\theta_{gr})$ are the values of shape parameter in the up and down swell directions respectively.
Then the modified model can be written as:

$$v_{low}(\theta_{gr}, \varphi_{sw}) = v_{sum}(\theta_{gr}) + v_{diff}(\theta_{gr}) \cos(2\varphi_{sw}) \quad (9)$$

B. Shape parameter at high grazing angle

The models described above are mainly applicable to grazing angles < 10°. The K distribution shape models covering the grazing angle range 0.1° - 45° at X-band are described in [13]. In addition, the models cover both horizontal and vertical polarizations, any wind direction, sea states 2-6 and a wide range of radar resolved areas.
Also, the resulting estimates of fitted shape parameter ν as a function of grazing angle (5°, 10°, 15°, 20° and 25°) based on X-band radar sea clutter measurements from Low-Medium Grazing Angles Recorded from a Helicopter Platform [14] are shown in Figure 6. When computing the median of the fitted shape parameter, a weak increasing trend in v is observed as plotted with the dotted lines.

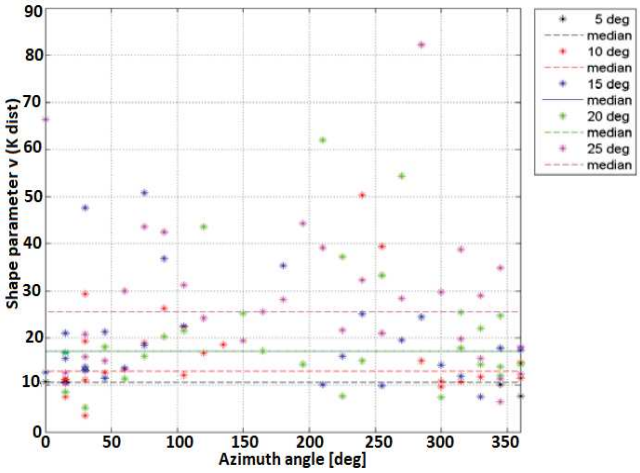

Fig. 6 Fitted shape parameter as a function of grazing and azimuth angle (reproduced from [14])

While Figure 7 shows an example of the shape parameter as a function of grazing angle between 15°-45° for the two separate Ingara trials. It illustrates the results obtained by Crisp at al. [15], that they undertook further analysis of the Ingara data previously reported by Dong [16] and also data from later Ingara trials. This work analysed a much larger data set and found more evidence of a dependence for ν on wind direction and grazing angle.

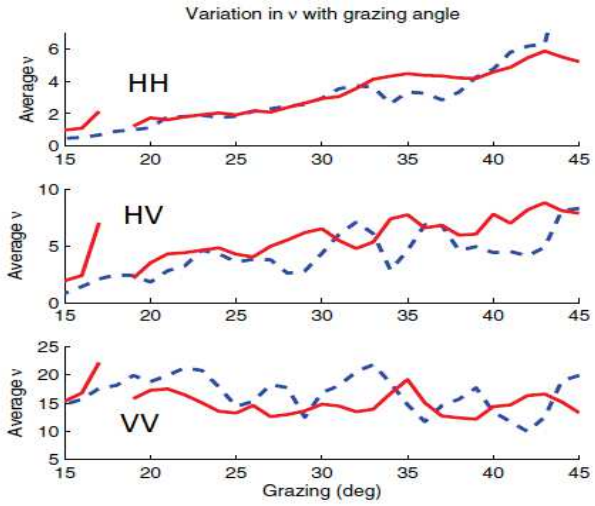

Fig. 7 Variation of shape parameter with grazing angle from Ingara. Red solid lines and blue dashed lines represent results from two data-gathering campaigns [15]

In this Figure, the discontinuities are due to missing data. The smaller values of ν occur at the lower grazing angle with HH data. It has been found that among the VV, HH, and HV polarizations, the VV data is least spiky compared to the HH and HV data.

C. *Scale parameter*

The scale parameter b is linked with the power of the clutter and represents the characteristics of the returned signal. The smaller the value of b the more powerful the reflected signal is from the sea surface and this can be predicted from the knowledge of the mean clutter reflectivity and the radar parameters.

$$P_c = \frac{v}{b} \quad (10)$$

The mean power of sea clutter is given by

$$P_c = \frac{P_t \mu_c G^2 \lambda^2 \sigma^0 A_c}{(4\pi)^3 R^4 L_a L_s} \quad (11)$$

Here, P_t is the transmitted power, μ_c is the pulse compression gain, G is the antenna gain, λ is the transmitted wavelength, R is the range from the radar to the target, σ^0 is the normalized sea clutter RCS, A_c is the area of illumination, L_a is the atmospheric and propagation loss, and L_s is the system loss. So, the scale parameter can be expressed as a function of the shape parameter and the received mean level power of sea clutter P_c:

$$b = \frac{(4\pi)^3 R^4 L_a L_s}{P_t \mu_c G^2 \lambda^2 \sigma^0 A_c} . v \quad (12)$$

IV. SIMULATION OF IMPACT OF DIFFERENT SHAPE VALUES ON SEA CLUTTER SPIKINESS

The K distributed samples were simulated independently by using the method introduced in [11], and the number of samples is 1000. According to simulation results, the feature of the impact of shape parameter values can be obtained. The shape parameter provides a measure of the amplitude spikiness; the smaller the value of ν, the sea clutter amplitude is spikier. So, in high grazing angle, especially at HH polarization when ν takes smaller values than lower grazing angle and VV polarization, the sea clutter becomes less spiky. To better understand how an increase in spikiness effects the statistics of the clutter we provide Figure 8 that compares three different levels of amplitude backscatter using simulated data with unit mean. Fig. 8(a) depicts very spiky clutter, Fig. 8(b) spiky clutter, whereas Fig. 8(c) shows clutter that is less spiky.

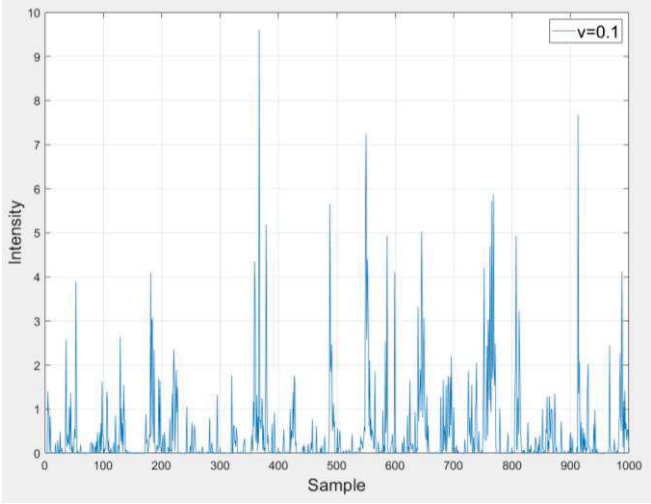

(a)

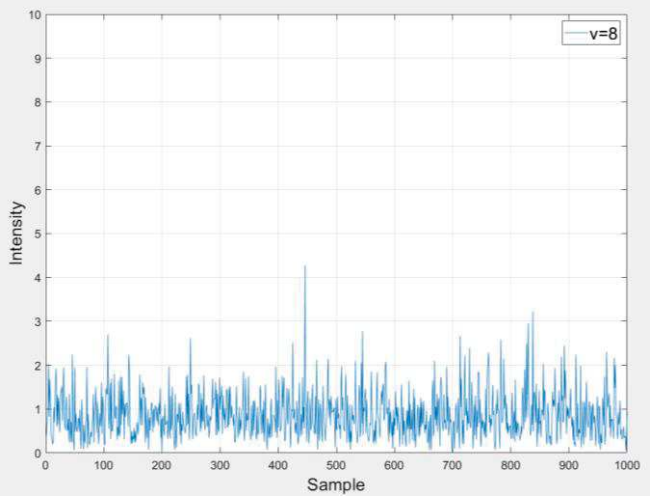

(b)

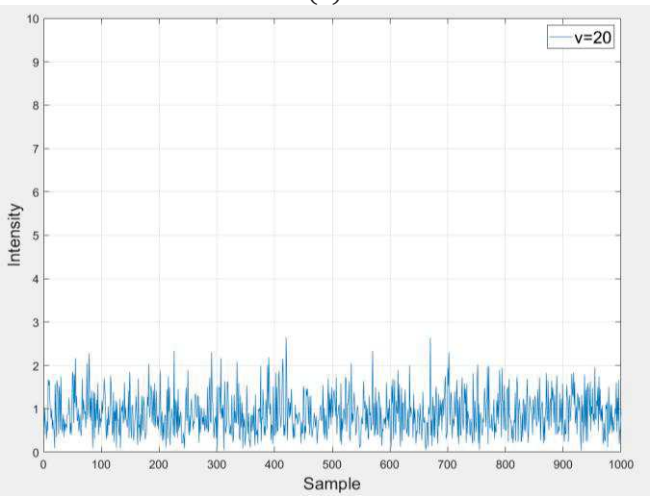

(c)

Fig. 8 K distribution random variates for different values of shape parameter ν with b= 1

V. CONCLUSION

Radar located on UAV at high altitude views the sea surface at much higher grazing angles (typically above 10 °), than ship or coastal radars. Since the dominant scattering mechanisms in sea clutter at low and high grazing angles are different, it would not be surprising if the nature and characteristics of the corresponding sea clutter are also different. So, this paper has briefly summarized the current literature on high grazing angle sea-clutter. The impact of high grazing angle normalized sea clutter is studied, and it can be seen that the detection of maritime targets on high grazing becomes more complex than on low grazing angle. At least, Analysis of the polarimetric behavior of sea clutter has suggested that at high grazing angles, an HH polarized radar outperforms a VV polarized radar in terms of target detection. Also, the main focus is on the estimation of the K distribution's shape parameter ν that provides a measure of the amplitude spikiness and plays a key role in the airborne radar applications.

In the context of study and analysis of the observation by a drone of the sea surface in the presence of naval targets, this work should continue with the integration and taking into account of sea clutter in a practical chain including functions of detection, localization and tracking of targets present in the area of interest.

REFERENCES

[1] C.Y.Chang, A. Woo, H. Forry, J. Sherman, M. Rechet, R. Clark, and R. Levin, "HISAR-300: An advanced airborne multi-mission surveillance radar," in Proc. IEEE Radar Conf.(RadarConf), Boston, MA, USA, Apr. 2019,pp.1_6.

[2] S. Liu, Y. Ma, and Y. Huang, "Sea clutter cancellation for passive radar sensor exploiting multi-channel adaptive filters," IEEE Sensors J., vol. 19, no. 3, pp. 982_995, Feb. 2019.

[3] I. Antipov. "Simulation of Sea Clutter Returns". DSTO-TR-0679 report,1998

[4] LONG, M.W.: 'Radar reflectivity of land and sea' (Artech House,1983)

[5] F.E. Nathanson, Radar Design Principles, McGraw Hill, 1969.

[6] Technology Service Corporation, "Backscatter from sea," Radar Workstation, vol. 2, pp. 177-186, 1990.

[7] F. T. Ulaby, et al., Microwave Remote Sensing: Active and Passive, Volume II: Radar Remote Sensing and Surface Scattering and Emission Theory: Addison-Wesley, 1982.

[8] V. Gregers-Hansen and R. Mittal, "An improved empirical model for radar sea-clutter reflectivity," IEEE Transaction on Aerospace and Electronic Systems, vol. 48, pp. 3512–3524, 2012.

[9] E. Jakeman and P. Pusey, "A model for non-rayleigh sea echo," IEEE Transactions on Antennas and Propagation, vol. 24, no. 6, pp. 806–814, November 1976.

[10] K. D. Ward, 'Compound representation of high resolution sea clutter', Electron. Lett., 17(16), 561-563, 1981

[11] K. D. Ward, R. J. A. Tough, and S. Watts, Sea Clutter: Scattering, the K-Distribution and Radar Performance, 2nd ed. The Institute of Engineering Technology, 2013.

[12] S. Watts and D. C. Wicks, "Empirical models for detection prediction in K-distribution sea clutter," in IEEE International Radar Conference, May 1990, pp. 189–194.

[13] L. Rosenberg, S. Watts "Continuous sea clutter models for the mean backscatter and k-distribution shape", Defence science and Technology Group, Australia

[14] T.Johnsen, N.Odegaard and A.O. Knapskog " X-Band Radar Sea-Clutter Measurements from Low-Medium Grazing Angles Recorded from a Helicopter Platform", Norwegian Defense Research Establishment

[15] D. J. Crisp,L. Rosenberg, N.J. Stacy "Modelling X-band Sea-Clutter with the K distribution: Shape Parameter Variation," in IEEE International Radar Conference, 2009

[16] Y. Dong, "Distribution of X-Band High Resolution and High Grazing Angle Sea-clutter," DSTO, Research Report DSTO-RR-0316, 2006.